JACS
JOURNAL OF THE AMERICAN CHEMICAL SOCIETY
Cite This: J. Am. Chem. Soc. XXXX, XXX, XXX−XXX
Communication
pubs.acs.org/JACS

Isotropic Effective Spin-Orbit Coupling in a Conjugated Polymer

Gajadhar Joshi,[†] Mandefro Y. Teferi,[†] Richards Miller,[†] Shirin Jamali,[†] Douglas Baird,[†] Johan van Tol,[‡] Hans Malissa,[†] John M. Lupton,*[,†,⊥] and Christoph Boehme*[,†]

[†]Department of Physics and Astronomy, University of Utah, 115 S, 1400 E, Salt Lake City, Utah 84112, United States
[‡]National High Magnetic Field Laboratory, Florida State University, Tallahassee, Florida 32310, United States
[⊥]Institut für Experimentelle und Angewandte Physik, Universität Regensburg, Universitätsstrasse 31, 93040 Regensburg, Germany

Supporting Information

ABSTRACT: Conjugated polymers are anisotropic in shape and with regard to electronic properties. Little is known as to how electronic anisotropy impacts the underlying characteristics of the electron spin, such as the coupling to orbital magnetic moments. Using multi-frequency electrically detected magnetic resonance spectroscopy extending over 12 octaves in frequency, we explore the effect of spin-orbit coupling by examining the pronounced broadening of resonance spectra with increasing magnetic field. Whereas in three commonly used materials, the high-field spectra show asymmetric broadening, as would be expected from anisotropic *g*-strain effects associated with the molecular structure, in the conducting polymer poly(3,4-ethylenedioxythiophene) polystyrene sulfonate (PEDOT:PSS) the spectra broaden isotropically, providing a direct measure of the microscopic distribution in *g*-factors. This observation implies that effective charge-carrier *g*-tensors are isotropic, which likely originates from motional narrowing in this high-mobility material.

Π-conjugated polymers are highly anisotropic. The most extreme cases of polydiacetylene can form almost perfectly one-dimensional structures extending over micrometers.[1] But even in less-ordered polymers, anisotropy can have dramatic effects on electronic properties, for example in organic light-emitting diodes (OLEDs), where oriented polymer films generate polarized light.[2] Little is known about how molecular anisotropy impacts the spin degree of freedom of charge-carriers. Spin plays a crucial role in the recombination of oppositely charged carriers in an OLED, but can also control transport properties, for example if doubly charged species such as bipolarons arise.[3] The spin of an electron on a molecule is influenced by two fundamental interactions: the coupling to nuclear magnetic moments, the hyperfine interaction, and the coupling to the orbital angular momentum of the electron wave function, spin-orbit coupling (SOC). In recent years, interest focused on exploiting hyperfine coupling in magnetic-field sensors,[4,5] exploring these magnetic field-dependent processes in detail by resolving hyperfine field-induced spin precession in time-resolved electron spin resonance (ESR) experiments[6] and controlling the interactions by changing molecular conformation and isotopic composition.[5,6] Assessing the influence of SOC in such materials has proven much more challenging,[7] even though the effect is crucial to device performance. In an OLED, for example, enhancing SOC by adding heavy nuclei mixes singlet and triplet spin states and allows radiative recombination to occur from the triplet as phosphorescence. As a result, OLEDs incorporating materials with strong SOC are more efficient than devices with pure singlet emitters.[8] But what role, if any, does SOC play in pure organic materials without heavy atoms?[9] Addressing this question is challenging, and previous work has focused primarily on photoinduced absorption studies of triplet exciton formation by excited-state intersystem crossing,[10] or on intrinsic phosphorescence.[11] However, there is no reason to assume that isolated charge carriers experience the same level of SOC as molecular excitons, which couple strongly to the molecular framework; in addition, assigning spectral features in photoinduced absorption can be challenging. The inverse spin-Hall effect, which measures a voltage build-up due to the separation of spin and charge, has emerged as an additional possibility of exploring SOC,[12] a relativistic effect controlling interconversion of electric and magnetic fields. The effect of SOC can be visualized by determining the correction to the magnetic moment of a free electron experienced under the influence of the orbital moment.[13] This perturbation is expressed by the electron *g*-factor, measured in ESR.[13] To do this necessitates operating at high resonance frequencies, where the distributions in local Zeeman splittings of the electron spin due to the SOC-induced variation in microscopic *g*-factors exceeds the local scatter in Zeeman splitting due to the hyperfine fields experienced by the spin.[14] Using a high-frequency ESR approach,[15] we compare resonance spectra of four commonly used π-conjugated polymers. The spectra broaden with increasing magnetic field, because the microscopic distribution in electronic *g*-factors broadens the range of possible energies for the Zeeman-split transitions as sketched in the inset of Figure 1a.

Poly(3,4-ethylenedioxythiophene) polystyrene sulfonate (PEDOT:PSS) is a widely used doped conducting polymer with a range of interesting morphological and electronic properties.[16] Ordering of the polymer chains can arise in the ensemble, so that different domains with a high degree of electronic delocalization emerge.[17] Because of the thiophene units on the polymer chain, somewhat stronger SOC than in pure organic compounds containing only hydrogen, carbon and

Received: March 22, 2018
Published: May 4, 2018

DOI: 10.1021/jacs.8b03069
J. Am. Chem. Soc. XXXX, XXX, XXX−XXX

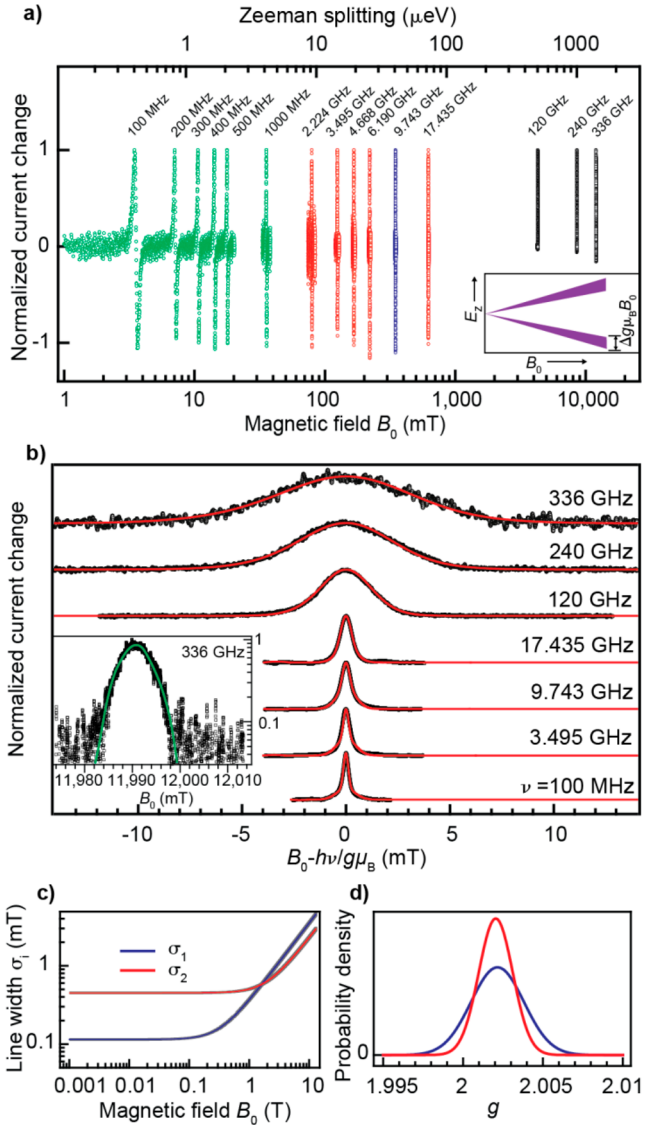

Figure 1. Frequency-dependent electrically detected magnetic resonance (EDMR) of PEDOT:PSS films. (a) EDMR spectra spanning over almost 12 octaves in radiation frequency. The three high-field spectra were measured under modulation of the radiation amplitude, whereas the low-field spectra were obtained by modulating the static magnetic field B_0, resulting in a derivative line shape. Green spectra were obtained with coils as RF source, red spectra used coplanar waveguides, the blue spectrum a commercial X-band resonator, and black spectra free-space millimeter-wave irradiation. The inset sketches the anticipated broadening of Zeeman sublevels due to the distribution of microscopic *g*-factors arising from SOC. (b) Spectral broadening with increasing frequency. The red curves show global double-Gaussian fits using the same parameter set for all frequencies. The inset plots the high-field spectrum on a logarithmic scale, demonstrating an isotropically broadened Gaussian (parabolic) line shape. A single Gaussian is superimposed. (c) Resonance spectral line widths of the two carriers of the pair extracted from global fits. (d) Corresponding distribution of *g*-factors for the two carrier species.

oxygen may be anticipated. This control of SOC has indeed been explored with conventional ESR,[18a,b] which, however, necessitates chemical doping of the material to form paramagnetic species and is usually carried out in solution.[18c] In a doped polymer, this approach is feasible and reasonable,[18d−f] but the spins observed may not be related to the current-carrying charge in a device. An alternative approach allows direct detection of charges' magnetic resonance signatures in an active device by recording current changes due to spin-dependent recombination.[19] When positive and negative charges annihilate by recombining, the device current changes. Owing to Pauli's principle, this recombination is inherently spin dependent so that changes in spin orientation of either electron or hole by magnetic resonance are mapped directly onto the current. This electrically detected magnetic resonance (EDMR) has proven both versatile and sensitive to probing spin interactions in operating devices based on molecular materials. Interestingly, even though PEDOT:PSS is *p*-doped and used as a hole-injection layer in OLEDs, the underlying polythiophene material still supports an electron minority-charge current so that spin-dependent recombination shows up both in EDMR[20] and in magnetoresistance.[21] We previously demonstrated that EDMR spectra are primarily broadened by hyperfine fields at low resonance frequencies, an effect that can be tested by replacing hydrogen with deuterium.[6] To conclusively establish the influence of SOC therefore requires measuring at different Zeeman splittings, i.e., at different external magnetic field strengths and resonance frequencies.[22]

Figure 1a shows continuous wave (c.w.) EDMR spectra measured on a PEDOT:PSS film at 5 K in an OLED geometry, i.e., with indium-tin oxide (ITO) and aluminum contacts.[20,22] The experimental spectra extend over almost 12 octaves in frequency. To span such a range requires a combination of different approaches. For frequencies up to 1 GHz, the radio frequency (RF) radiation can be delivered to the device using RF coils (green spectra).[23] For frequencies up to 20 GHz, coplanar waveguide resonators are used as the source of RF radiation (red).[22] The spectrum at 9.74 GHz was obtained in a commercial X-band microwave resonator (blue).[20] Spectra above 100 GHz were acquired in a high-field setup[15] under free-space irradiation with millimeter waves (black). The spectra up to 17.4 GHz were recorded by modulating Zeeman splitting, i.e., the B_0 field, which gives the resonance a derivative line shape. At high fields, it is easier to modulate radiation amplitude rather than magnetic field, so that the resonances acquire integral form. To compare the two types of spectra, we integrate the low-frequency derivative spectra and plot these in panel b. As the frequency increases, the spectra broaden 25-fold from 0.32 mT width to 7.96 mT. At low fields, the spectra are described accurately by a superposition of two Gaussians, one for the hyperfine distribution experienced by the hole, the other for the electron.[14,23,24] At the highest field of 12 T, however, the spectrum resembles a single Gaussian, a perfect parabola on the semilogarithmic scale in the inset (green). This observation implies that at the highest fields, when the spectral shape is dominated solely by SOC and the resulting distribution of microscopic *g*-factors, the effective SOC must be isotropic. Because the other spectra can only be described by the sum of two Gaussians, a multidimensional fit with statistical analysis must be employed in order to obtain the parameters of line broadening with field.[24]

Following the earlier procedure for analyzing multifrequency EDMR spectra,[14,22b] the red lines in Figure 1b show global fits for all data sets simultaneously using the same constant Gaussian distribution of hyperfine fields for the two spins, along with an additional field-dependent spectral broadening mechanism. This fit reveals a narrow and a broad field-independent hyperfine distribution, $\Delta B_{hyp,1}$ and $\Delta B_{hyp,2}$, which contribute to the overall field-dependent line width. For each of

DOI: 10.1021/jacs.8b03069
J. Am. Chem. Soc. XXXX, XXX, XXX−XXX

the two spins, this line width is $\sigma_i(B_0) = \sqrt{\Delta B_{\mathrm{hyp},i}^{\ 2} + \alpha_i^{\ 2} B_0^{\ 2}}$, where α is a constant for each spin describing the influence of field-dependent spectral broadening due to the g-strain, i.e., the distribution of g-factors. No assignment is made of the two resonance constituents to electron or hole, which is unnecessary for the discussion.

The results of the global fit[24] are plotted in panel b (red lines) and the resulting field-dependent line widths are shown in panel c, with the corresponding parameters listed in Table S1 of the Supporting Information.[24] Spectral broadening due to g-strain becomes discernible above 100 mT and appears to be stronger for one of the two resonant species. The distributions of microscopic g-factors for both spins are plotted in Figure 1d on the basis of this global fit result. Note that these plots represent normalized probability distributions and do not show the intensity of the two resonances.

SOC in PEDOT:PSS induces symmetric spectral broadening at high magnetic fields, giving rise to a single dominant Gaussian line shape emerging from the double-Gaussian structure of the spectrum. Such behavior is not intuitively reconciled with structural anisotropy. We compare PEDOT:PSS with three other common conjugated polymer materials, poly[9,9-dioctylfluorenyl-2,7-diyl] (PFO) in its glassy morphology, poly[2-methoxy-5-(2-ethylhexyloxy)-1,4-phenylenevinylene] (MEH-PPV),[15] and the commercial proprietary "super-yellow" PPV (SYPPV). Figure 2 shows EDMR spectra for the four materials at 4 and 8 T. Note that because EDMR signals are detectable in PEDOT:PSS at low temperatures only, we recorded these spectra at 5 K; the remainder were measured at room temperature. The red lines show the results of the same global fitting procedure discussed in Figure 1. The complete frequency-dependent data sets are given in the Supporting Information.[24] At the two frequencies shown, only the PEDOT:PSS spectra can be fitted by a common set of parameters. The other spectra exhibit a varying degree of asymmetry, which can be directly related to the anisotropy in SOC and the resulting anisotropic g-tensor. In a recent comparison of g-tensor calculations from density-functional theory, we were able to replicate the anisotropic line shape of MEH-PPV.[15]

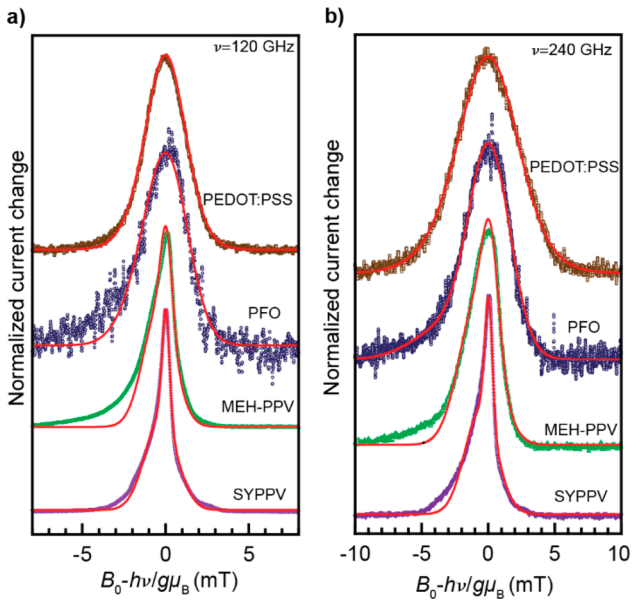

Figure 2. Comparison of high-field EDMR spectra for different conjugated polymers at 4 T (a) and 8 T (b). The red lines show the results of double-Gaussian global fits to the spectra measured at all frequencies, using a common parameter set, i.e., a fixed hyperfine distribution for the two spins of the pair (see Supporting Information for complete data sets). As discussed in Ref 14, these double-Gaussian fits are clearly inappropriate. Only PEDOT:PSS shows symmetric resonances, implying that the effective SOC is anisotropic in the other materials.

PEDOT:PSS shows much stronger spectral broadening with increasing field than other conjugated polymers, implying that the effective SOC must be substantially larger. This increased SOC likely arises from the thiophenes in PEDOT:PSS.[18c] However, at low fields, the PEDOT:PSS spectra are narrower than those of the other three materials because random hyperfine fields are weak owing to the comparative sparsity of hydrogen nuclei; at higher fields, the effect of SOC dominates so that the PEDOT:PSS spectra become much broader than those of the other materials. We conclude by hypothesizing on the possible origins of the apparent isotropic SOC effect in PEDOT:PSS. Because EDMR probes spin-dependent transitions, motion of the carriers within the molecular framework may change the effective spin interaction, both hyperfine coupling and SOC, a phenomenon known as motional narrowing. Evidence relating to resonance line widths and spin coherence times exists that this effect occurs in conjugated polymers, reducing effective hyperfine-coupling strengths.[25,26] In PEDOT:PSS, where microcrystalline domains with a high degree of interchain mobility exist,[17a,c] the charges may move so swiftly between the anisotropic molecular building blocks that the anisotropic influence of the SOC is averaged out. Such microstructure formation is particularly prevalent in the capacitive device geometries studied here, where two phases of either PEDOT-rich or PSS-rich domains are thought to arise.[27] The fact that the spectral complexity decreases with increasing magnetic field strength, leading to the single dominating Gaussian line shape, could be a result of the high mobility of charge carriers in PEDOT-rich domains of this material. Combined measurements of spin coherence times by spin-echo spectroscopy[25,26] with SOC-induced spectral broadening could therefore offer a route to probing nanoscale ballistic transport, because spectral broadening should relate to the transport time scales. Future work should be directed at correlating SOC-broadening with carrier mobility, which can be controlled by doping and manipulation of chain morphology.[26] Finally, we note that in most conjugated-polymer materials, SOC appears to have a non-negligible contribution to resonance line shape even at X-band frequencies, an effect that has previously been mostly overlooked. Caution is therefore called for when inferring the delocalization of polaron wave functions from hyperfine motional-narrowing effects alone.[28]

■ ASSOCIATED CONTENT

Supporting Information

The Supporting Information is available free of charge on the ACS Publications website at DOI: 10.1021/jacs.8b03069.

Multifrequency EDMR of different conjugated polymers; experimental methods; details on the global fitting procedure and the statistical bootstrap analysis for determining confidence intervals of fit parameters (PDF)

DOI: 10.1021/jacs.8b03069
J. Am. Chem. Soc. XXXX, XXX, XXX−XXX

AUTHOR INFORMATION

Corresponding Authors

*john.lupton@ur.de
*boehme@physics.utah.edu

ORCID

Hans Malissa: 0000-0002-5964-3225
John M. Lupton: 0000-0002-7899-7598
Christoph Boehme: 0000-0001-7323-5757

Notes

The authors declare no competing financial interest.

ACKNOWLEDGMENTS

This work was supported by the U.S. Department of Energy, Office of Basic Energy Sciences, Division of Materials Sciences and Engineering under Award #DE-SC0000909. Part of this work was performed at the National High Magnetic Field Laboratory, which is supported by National Science Foundation Cooperative Agreement No. DMR-1157490 and the State of Florida.

REFERENCES

(1) Dubin, F.; Melet, R.; Barisien, T.; Grousson, R.; Legrand, L.; Schott, M.; Voliotis, V. *Nat. Phys.* **2006**, *2* (1), 32−35.

(2) Grell, M.; Knoll, W.; Lupo, D.; Meisel, A.; Miteva, T.; Neher, D.; Nothofer, H. G.; Scherf, U.; Yasuda, A. *Adv. Mater.* **1999**, *11* (8), 671−675.

(3) Bobbert, P. A.; Nguyen, T. D.; van Oost, F. W. A.; Koopmans, B.; Wohlgenannt, M. *Phys. Rev. Lett.* **2007**, *99* (21), 216801.

(4) Wagemans, W.; Koopmans, B. *Phys. Status Solidi B* **2011**, *248* (5), 1029−1041.

(5) Nguyen, T. D.; Hukic-Markosian, G.; Wang, F. J.; Wojcik, L.; Li, X. G.; Ehrenfreund, E.; Vardeny, Z. V. *Nat. Mater.* **2010**, *9* (4), 345−352.

(6) Malissa, H.; Kavand, M.; Waters, D. P.; van Schooten, K. J.; Burn, P. L.; Vardeny, Z. V.; Saam, B.; Lupton, J. M.; Boehme, C. *Science* **2014**, *345* (6203), 1487−1490.

(7) (a) Barford, W.; Bursill, R. J.; Makhov, D. V. *Phys. Rev. B: Condens. Matter Mater. Phys.* **2010**, *81* (3), 035206. (b) Beljonne, D.; Shuai, Z.; Pourtois, G.; Brédas, J. L. *J. Phys. Chem. A* **2001**, *105* (15), 3899−3907. (c) Harmon, N. J.; Flatté, M. E. *Phys. Rev. Lett.* **2013**, *110* (17), 176602. (d) Nuccio, L.; Willis, M.; Schulz, L.; Fratini, S.; Messina, F.; D'Amico, M.; Pratt, F. L.; Lord, J. S.; McKenzie, I.; Loth, M.; Purushothaman, B.; Anthony, J.; Heeney, M.; Wilson, R. M.; Hernandez, I.; Cannas, M.; Sedlak, K.; Kreouzis, T.; Gillin, W. P.; Bernhard, C.; Drew, A. J. *Phys. Rev. Lett.* **2013**, *110* (21), 216602. (e) Rybicki, J.; Wohlgenannt, M. *Phys. Rev. B: Condens. Matter Mater. Phys.* **2009**, *79* (15), 153202. (f) Yu, Z. G. *Phys. Rev. B: Condens. Matter Mater. Phys.* **2012**, *85* (11), 115201.

(8) Baldo, M. A.; O'Brien, D. F.; You, Y.; Shoustikov, A.; Sibley, S.; Thompson, M. E.; Forrest, S. R. *Nature* **1998**, *395* (6698), 151−154.

(9) McClure, D. S. *J. Chem. Phys.* **1952**, *20*, 682.

(10) Cadby, A. J.; Yang, C.; Holdcroft, S.; Bradley, D. D. C.; Lane, P. A. *Adv. Mater.* **2002**, *14* (1), 57−60.

(11) (a) Chaudhuri, D.; Sigmund, E.; Meyer, A.; Rock, L.; Klemm, P.; Lautenschlager, S.; Schmid, A.; Yost, S. R.; Van Voorhis, T.; Bange, S.; Höger, S.; Lupton, J. M. *Angew. Chem., Int. Ed.* **2013**, *52*, 13449−13452. (b) Ratzke, W.; Schmitt, L.; Matsuoka, H.; Bannwarth, C.; Retegan, M.; Bange, S.; Klemm, P.; Neese, F.; Grimme, S.; Schiemann, O.; Lupton, J. M.; Höger, S. *J. Phys. Chem. Lett.* **2016**, *7*, 4802−4808. (c) Salas Redondo, C.; Kleine, P.; Roszeitis, K.; Achenbach, T.; Kroll, M.; Thomschke, M.; Reineke, S. *J. Phys. Chem. C* **2017**, *121*, 14946−14953.

(12) Ando, K.; Watanabe, S.; Mooser, S.; Saitoh, E.; Sirringhaus, H. *Nat. Mater.* **2013**, *12* (7), 622−627.

(13) (a) Elliott, R. J. *Phys. Rev.* **1954**, *96* (2), 266−279. (b) Segal, B. G.; Kaplan, M.; Fraenkel, G. K. *J. Chem. Phys.* **1965**, *43* (12), 4191−4200.

(14) (a) Burghaus, O.; Plato, M.; Rohrer, M.; Möbius, K.; Macmillan, F.; Lubitz, W. *J. Phys. Chem.* **1993**, *97* (29), 7639−7647. (b) Hassan, A. K.; Pardi, L. A.; Krzystek, J.; Sienkiewicz, A.; Goy, P.; Rohrer, M.; Brunel, L. C. *J. Magn. Reson.* **2000**, *142* (2), 300−312. (c) Akhtar, W.; Schnegg, A.; Veber, S.; Meier, C.; Fehr, M.; Lips, K. *J. Magn. Reson.* **2015**, *257*, 94−101. (d) Barra, A. L.; Brunel, L. C.; Robert, J. B. *Chem. Phys. Lett.* **1990**, *165* (1), 107−109.

(15) Malissa, H.; Miller, R.; Baird, D. L.; Jamali, S.; Joshi, G.; Bursch, M.; Grimme, S.; van Tol, J.; Lupton, J. M.; Boehme, C. *Phys. Rev. B: Condens. Matter Mater. Phys.* **2018**, *97*, 161201.

(16) (a) Kirchmeyer, S.; Reuter, K. *J. Mater. Chem.* **2005**, *15* (21), 2077−2088. (b) Frohne, H.; Müller, D. C.; Meerholz, K. *ChemPhysChem* **2002**, *3* (8), 707−711. (c) Bubnova, O.; Khan, Z. U.; Malti, A.; Braun, S.; Fahlman, M.; Berggren, M.; Crispin, X. *Nat. Mater.* **2011**, *10* (6), 429−433. (d) Bubnova, O.; Khan, Z. U.; Wang, H.; Braun, S.; Evans, D. R.; Fabretto, M.; Hojati-Talemi, P.; Dagnelund, D.; Arlin, J. B.; Geerts, Y. H.; Desbief, S.; Breiby, D. W.; Andreasen, J. W.; Lazzaroni, R.; Chen, W. M. M.; Zozoulenko, I.; Fahlman, M.; Murphy, P. J.; Berggren, M.; Crispin, X. *Nat. Mater.* **2014**, *13* (2), 190−194.

(17) (a) Nardes, A. M.; Kemerink, M.; Janssen, R. A. J.; Bastiaansen, J. A. M.; Kiggen, N. M. M.; Langeveld, B. M. W.; van Breemen, A.; de Kok, M. M. *Adv. Mater.* **2007**, *19* (9), 1196−1200. (b) Lang, U.; Müller, E.; Naujoks, N.; Dual, J. *Adv. Funct. Mater.* **2009**, *19* (8), 1215−1220. (c) Kang, K.; Watanabe, S.; Broch, K.; Sepe, A.; Brown, A.; Nasrallah, I.; Nikolka, M.; Fei, Z. P.; Heeney, M.; Matsumoto, D.; Marumoto, K.; Tanaka, H.; Kuroda, S.; Sirringhaus, H. *Nat. Mater.* **2016**, *15* (8), 896−902.

(18) (a) Zykwinska, A.; Domagala, W.; Czardybon, A.; Pilawa, B.; Lapkowski, M. *Chem. Phys.* **2003**, *292* (1), 31−45. (b) Lee, J. K.; You, S.; Jeon, S.; Ryu, N. H.; Park, K. H.; Myung-Hoon, K.; Kim, D. H.; Kim, S. H.; Schiff, E. A. *J. Appl. Phys.* **2015**, *118* (1), 015501. (c) Schott, S.; McNellis, E. R.; Nielsen, C. B.; Chen, H. Y.; Watanabe, S.; Tanaka, H.; McCulloch, I.; Takimiya, K.; Sinova, J.; Sirringhaus, H. *Nat. Commun.* **2017**, *8*, 15200. (d) Cravino, A.; Neugebauer, H.; Luzzati, S.; Catellani, M.; Petr, A.; Dunsch, L.; Sariciftci, N. S. *J. Phys. Chem. B* **2002**, *106* (14), 3583−3591. (e) Kanemoto, K.; Muramatsu, K.; Baba, M.; Yamauchi, J. *J. Phys. Chem. B* **2008**, *112* (35), 10922−10926. (f) Ling, Y.; Van Mierloo, S.; Schnegg, A.; Fehr, M.; Adriaensens, P.; Lutsen, L.; Vanderzande, D.; Maes, W.; Goovaerts, E.; Van Doorslaer, S. *Phys. Chem. Chem. Phys.* **2014**, *16* (21), 10032−10040.

(19) Graeff, C. F. O.; Brandt, M. S.; Faria, R. M.; Leising, G. *Phys. Status Solidi A-Appl. Res.* **1997**, *162* (2), 713−721.

(20) van Schooten, K. J.; Baird, D. L.; Limes, M. E.; Lupton, J. M.; Boehme, C. *Nat. Commun.* **2015**, *6*, 6688.

(21) (a) Klemm, P.; Bange, S.; Pollmann, A.; Boehme, C.; Lupton, J. M. *Phys. Rev. B: Condens. Matter Mater. Phys.* **2017**, *95* (24), 241407. (b) Aleshin, A. N.; Williams, S. R.; Heeger, A. J. *Synth. Met.* **1998**, *94* (2), 173−177.

(22) (a) Baker, W. J.; Ambal, K.; Waters, D. P.; Baarda, R.; Morishita, H.; van Schooten, K.; McCamey, D. R.; Lupton, J. M.; Boehme, C. *Nat. Commun.* **2012**, *3*, 898. (b) Joshi, G.; Miller, R.; Ogden, L.; Kavand, M.; Jamali, S.; Ambal, K.; Venkatesh, S.; Schurig, D.; Malissa, H.; Lupton, J. M.; Boehme, C. *Appl. Phys. Lett.* **2016**, *109* (10), 103303.

(23) Waters, D. P.; Joshi, G.; Kavand, M.; Limes, M. E.; Malissa, H.; Burn, P. L.; Lupton, J. M.; Boehme, C. *Nat. Phys.* **2015**, *11* (11), 910−914.

(24) See Supporting Information for further details.

(25) Baker, W. J.; Keevers, T. L.; Lupton, J. M.; McCamey, D. R.; Boehme, C. *Phys. Rev. Lett.* **2012**, *108* (26), 267601.

(26) Teferi, M. Y.; Ogle, J.; Joshi, G.; Malissa, H.; Jamali, S.; Baird, D. L.; Lupton, J. M.; Whittaker Brooks, L.; Boehme, C. *arXiv.org e-Print archive*. http://arxiv.org/abs/1804.05139 (accessed May 16, 2018).

DOI: 10.1021/jacs.8b03069
J. Am. Chem. Soc. XXXX, XXX, XXX−XXX

(27) Volkov, A. V.; Wijeratne, K.; Mitraka, E.; Ail, U.; Zhao, D.; Tybrandt, K.; Andreasen, J. W.; Berggren, M.; Crispin, X.; Zozoulenko, I. V. *Adv. Funct. Mater.* **2017**, *27* (28), 1700329.
(28) (a) Marumoto, K.; Kuroda, S.; Takenobu, T.; Iwasa, Y. *Phys. Rev. Lett.* **2006**, *97* (25), 256603. (b) Rawson, J.; Angiolillo, P. J.; Therien, M. J. *Proc. Natl. Acad. Sci. U. S. A.* **2015**, *112* (45), 13779–13783.

DOI: 10.1021/jacs.8b03069
J. Am. Chem. Soc. XXXX, XXX, XXX−XXX